Thermal donors formation via isothermal annealing in magnetic Czochralski high resistivity silicon

Mara Bruzzi,[a] David Menichelli, and Monica Scaringella
INFN Firenze and Dipartimento di Energetica, Università di Firenze, via S. Marta 3, 50139 Florence, Italy

Jaakko Härkönen and Esa Tuovinen
Helsinki Institute of Physics, University of Helsinki, Gustaf Hällströmin katu 2, FIN-00014, Finland

Zheng Li
Brookhaven National Laboratory, Instrumentation Division, 535B, 20N Technology Street, Upton, New York 11973-5000

(Received 12 October 2005; accepted 8 February 2006; published online 12 May 2006)

A quantitative study about the thermal activation of oxygen related thermal donors in high resistivity *p*-type magnetic Czochralski silicon has been carried out. Thermal donor formation has been performed through isothermal annealing at 430 °C up to a total time of 120 min. Space charge density after each annealing step has been measured by transient current technique. The localized energy levels related to thermal double donors (TD) have been observed and studied in details by thermally stimulated currents (TSCs) in the range of 10–70 K, and activation energies E and effective cross sections σ have been determined for both the emissions $TD^{0/+}$ (E=75±5 meV, σ $=4\times10^{-14}$ cm^2) and $TD^{+/+}$ (E=170±5 meV, $\sigma=2\times10^{-12}$ cm^2). The evolution of the space charge density caused by annealing has been unambiguously related to the activation of TDs by means of current deep level transient spectroscopy TSC, and current transients at constant temperature $i(t,T)$. Our results show that TDs compensate the initial boron doping, eventually provoking the sign inversion of the space charge density. TD's generation rate has been found to be linear with the annealing time and to depend critically on the initial interstitial oxygen concentration, in agreement with previous models developed on low resistivity silicon. © *2006 American Institute of Physics*.
[DOI: 10.1063/1.2192307]

I. INTRODUCTION

Float zone (FZ) silicon is used in several applications where a semiconductor material with both high crystalline quality and high resistivity is required.[1–3] Recently, Czochralski (Cz) silicon with high crystalline quality and resistivity of the order of 1 $k\Omega$ cm has become commercially available.[4–6] The growth procedure can include the application of an external magnetic field to stabilize the melt flow during the crystal growth, thus improving the crystal quality and yields.[7] In this case the material is called magnetic Czochralski (MCz) silicon.

In the Cz technique silicon is grown in a quartz crucible,[5] and the material is naturally enriched with interstitial oxygen (O_i), which is present in concentrations up to $[O_i]\sim10^{18}$ cm^{-3} (while in float zone, $[O_i]\sim10^{15}$ cm^{-3}). It is well known that in oxygen enriched silicon ($[O_i]$ $>10^{17}$ cm^{-3}) the formation of a significant amount of thermal double donors (usually indicated as TD or TDD) may occur. TDs are small clusters of atoms formed at the early stages of oxygen aggregation.[8–10] It has been widely shown that in Cz silicon TDs formation is activated by heat treatments in the temperature range of 400–500 °C.[11–13] Shallow thermal donors (STD) with ionization energies in the range of 30–40 meV can be activated in the same temperature range[14] too. STDs are believed to have a structure similar to TD, but incorporate a hydrogen atom or other impurities.

Formation of thermal donors is a critical issue in high resistivity Cz Si. In fact, the concentration of TDs generated by typical processing temperatures of microelectronic devices can be high enough to critically change the local resistivity along the wafer.[15] Nonetheless, up to now the problem of TD formation has been studied mainly only in low resistivity (typically 1–100 Ω cm) Cz silicon.[11,12]

This paper reports a quantitative study of TD activation in MCz samples with resistivity ranging from 1 $k\Omega$ cm to quasi-intrinsic. TDs activation has been performed through thermal treatments at 430 °C in six steps, up to a total time of 120 min. In Refs. 11 and 12, where the samples resistivity was typically of the order of 10 Ω cm, the TD concentration was determined by four-probe measurements at room temperature. Since this technique cannot detect a change of conductivity type, we simultaneously determined resistivity and conductivity type by transient current technique (TCT).[16] Starting with a high resistivity *p*-type material, an inversion of the conductivity type has been measured after the last annealing step.

In this work, the evolution of space charge density caused by annealing is unambiguously related to TDs activation by thermal spectroscopy techniques such as current deep level transient spectroscopy[17–19] (*I*-DLTS) and thermally stimulated currents (TSCs).[20] The TDs activation energies and effective cross sections[21] have been measured, and evi-

[a]Author to whom correspondence should be addressed; electronic mail: mara.bruzzi@unifi.it

 © 2006 American Institute of Physics

Downloaded 30 Jan 2007 to 192.84.145.254. Redistribution subject to AIP license or copyright, see http://jap.aip.org/jap/copyright.jsp

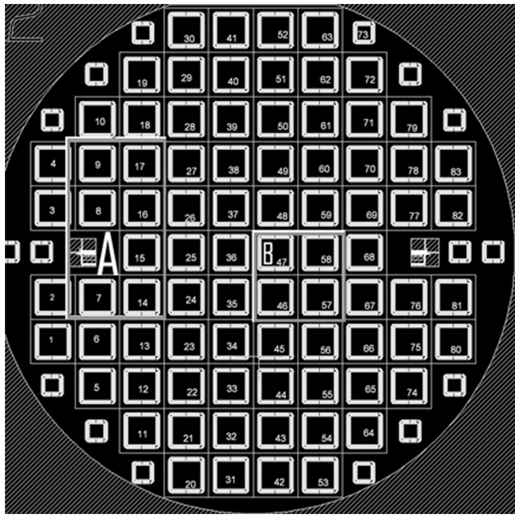

FIG. 1. Layout of the wafer processed at the Helsinki University of Technology Microelectronics Center to produce $p^+/p/n^+$ diodes from high resistivity magnetic Czochralski silicon. The six diodes used in this work are Nos. 7, 8, and 17 (from set A) and 46, 57, and 58 (from set B).

dence of Poole-Frenkel effect[22,23] is advantageously used to determine the charge state of these energy levels. Further information about the energy levels responsible for the space charge sign inversion are deduced from current transient measurements at constant temperature $i(t,T)$. Finally, the models of TD formation proposed in older works are discussed within the perspectives opened by our results.

II. EXPERIMENTAL PROCEDURE

The samples used in this study are $p^+/p/n^+$ devices (active area 0.25 cm^2, thickness W=300 μm) made from $\langle 100\rangle$ MCz p-type Si wafers by Okmetic, Finland, with a resistivity of about 1 $k\Omega$ cm. The diodes have been processed by the Helsinki University of Technology, Finland, from 4 in. wafers. Secondary-ion-mass spectroscopy (SIMS) measurements gave indication that $[O_i]\sim(4.6\pm0.2)\times10^{17}$ cm^{-3}.[24] The p^+ implant (boron) on front surface is surrounded by a set of guard rings, while the back n^+ contact is made with a P implant on the whole wafer surface. Two windows have been cut in the Al layer at back and front electrodes to allow optical excitation via a laser beam. The distribution of the six investigated diodes along the wafer size is shown in Fig. 1. The samples belong to two sets: diodes 7, 8, and 17 have been cut from the central part of the wafer (set A), while diodes 46, 57, and 58 have been cut from a peripheral region (set B).

Details about diode processing can be found in Ref. 15. After processing, an isothermal annealing has been performed using a nitrogen-controlled atmosphere oven, by heating all the diodes in different time periods ranging from 45 to 120 min at 430 °C. Heating treatments and TCT measurements have been performed at the Brookhaven National Laboratory, Upton, NY. After each annealing step, full depletion voltage V_{fd} and space charge concentration have been determined by TCT.[25] In the TCT setup the sample is ac coupled with a 500 MHz oscilloscope (Tektronix TDS-445) by a coaxial cable. Nonequilibrium carriers were generated on the surface of the crystal by laser pulses with 660 nm wavelength and about 1 ns duration. The diameter of the laser spot on the detector was about 2 mm. Laser pulses were flashed repeatedly either on the front or the rear contact, while a reverse voltage in the range of 0–400 V was applied to the device by means of a Keithley 238 I/V source.

TSC, I-DLTS, and $i(t,T)$ measurements have been performed at Dipartimento di Energetica, Università di Firenze (DEF), Italy. The experimental setup is described in details in Ref. 26. The sample is cooled by immersion in liquid helium vapor. The initial temperature is thus determined by the sample holder height above the He surface. A heating resistance, allocated inside the sample holder, increases the sample temperature during thermal scans. The temperature sensor is a silicon diode (Lake Shore DT-470-CU11), measured by a temperature controller (Lake Shore DRC91C). In I-DLTS and $i(t,T)$ experiments, the reverse bias V_{rev} and the forward voltage pulses V_p for sample excitation are provided by a pulse generator (Systron Donner 110D), and the current transients $i(t,T)$ are measured using a custom readout circuit. It converts the current into voltage, ensuring adequate values of transresistance (r=0.5–2 $10^6\times$V/A), input resistance (R_{in}=2.2 k Ω), and bandwidth (BWD=1 MHz). The readout circuit output is monitored by a 500 MHz digital oscilloscope (Tektronix TDS520D) which samples the current transients. During each current transient acquisition the temperature is kept constant. The I-DLTS spectra $S(T)$ are extracted from current transients as $S(T)=i(t_1,T)$-$i(t_2,T)$, where t_1 and t_2 are two fixed sampling times. In TSC experiments, reverse biasing and current reading are provided by a Keithley 6517 electrometer. During the excitation stage, a forward bias is applied to the diode in order to saturate the concentration of filled states.

III. EXPERIMENTAL RESULTS AND DISCUSSION

A. TCT measurements

The TCT technique has been used to determine the full depletion voltage (V_{fd}), the sign of the space charge ($\eta=\pm1$) and the effective doping concentration N_{eff}. According to this notation, the space charge density is $\rho=\eta N_{eff}$ (in elementary charges per unit volume). As an example, the results of the measurements carried out on one of the samples (no. 46) before any thermal treatment are reported in Fig. 2. The small picture inside the plots depicts a cross section of the device indicating the relative position of the laser beam and of the sample. Depletion region and electrodes are indicated by shaded and black areas, respectively. As the device is a $p^+/p/n^+$ junction ($\eta=-1$), the depletion region develops from the back electrode. When the reverse bias (V_{rev}) is increased, the depletion depth x_d increases as well, reaching the device thickness at full depletion. For this reason, when the laser is pulsed on the front electrode a significant charge is collected only when $V_{rev}\geqslant V_{fd}$ [Fig. 2(a)). On the contrary, a non-negligible charge collection is always measured when the laser is pulsed on the back electrode [Fig. 2(b)].

Figure 3 shows the collected charge Q, obtained by integrating the TCT current signal, as a function of V_{rev}. The linear fits (before and after full depletion) of the $Q(V_{rev})$

Downloaded 30 Jan 2007 to 192.84.145.254. Redistribution subject to AIP license or copyright, see http://jap.aip.org/jap/copyright.jsp

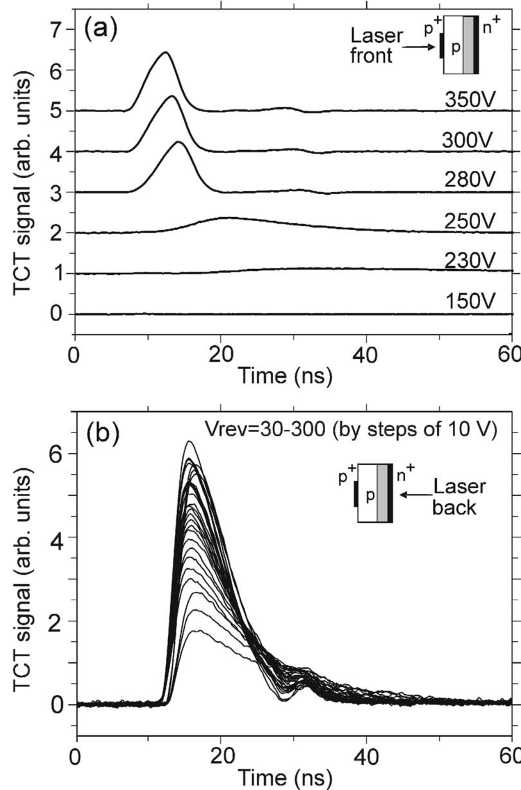

FIG. 2. TCT signals measured with sample 46 at different reverse biases. Laser is pulsed either on the front (a) or on the back (b) side of the sample.

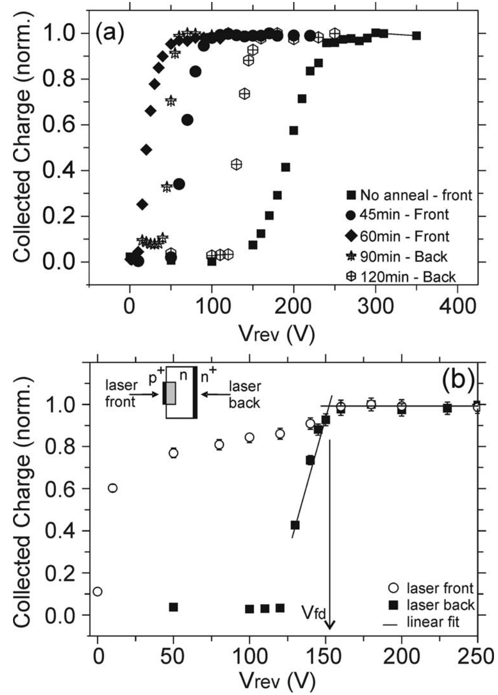

FIG. 4. (a) Charge collected with laser placed on back or front electrodes as a function of reverse voltage, (sample 46) after each annealing step at 430 °C. (b) Comparison of the charge collected with laser placed on back and front electrodes after the last annealing step (120 min). The charge has been normalized to the maximum value obtained for voltages higher than V_{fd}.

measurement carried out with the laser pulsing on the front side are shown too. V_{fd} is determined as the abscissa of the intersection point of these fits ($V_{fd}=233\pm5$ V for this sample). Prior to any thermal treatment no correlation has been found between N_{eff} and the position of the diode along the wafer. For all the samples we estimate a space charge density of $\rho=-(3.5\pm0.4)\times10^{12}$ cm^{-3}.

The TCT measurements have been repeated for each diode after five different annealing treatments at 430 °C. The total duration of these treatments were 0, 45, 60, 90, and 120 min. The charge collection measurements carried out on one of the samples (No. 46) are reported in Fig. 4(a). Before annealing and up to 60 min of annealing the total collected charge drops to zero if $V_{rev}<V_{fd}$ when laser hits the front

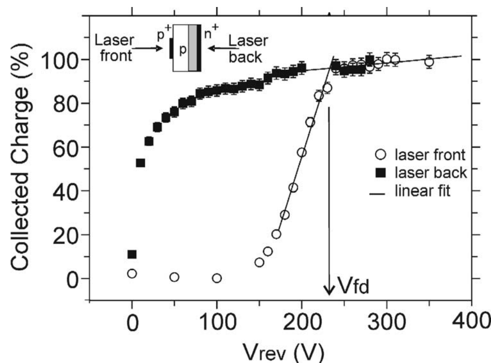

FIG. 3. Comparison of the charge collected with laser pulsing on back and front electrodes, as measured with sample 46, before the annealing treatment.

side, because the sign of the space charge is $\eta=-1$. A decrease of the full depletion voltage to values of the order of few volts can be easily explained considering that the annealing procedure activates TD energy levels, which compensate the shallow boron present in the starting material. Very high resistivity values, up to $\rho\sim10-30$ $k\Omega$ cm, are achieved in this way after 45–60 min of annealing. After annealing times of 90 and 120 min, the signal saturation at full depletion can be evidenced only if the laser beam hits the sample on the back side, as shown in Fig. 4(b). This indicates that the activated TD has overcompensated the boron doping, the conductivity type of the bulk has become n type ($\eta=+1$), and, correspondingly, the space charge region has shifted close to the front electrode. After the last annealing step (120 min) a positive space charge density ($\eta=+1$) is measured in all the six diodes.

Full depletion voltages measured by TCT for all the six diodes are shown in Fig. 5 as a function of the annealing time. We observe that samples which were close to each other along the wafer (see Fig. 1) exhibit a similar trend of V_{fd}: the final full depletion voltage values of the two groups A and B differ by about 100 V.

B. TSC and DLTS measurements

Emissions from localized energy levels have been studied by TSCs and I-DLTS, and the results of our analysis have been compared with literature. TD centers comprise a family of more than 16 double donors.[13,27] However, DLTS is unable to resolve the energy levels of individual TD species. As a consequence, only two TD-related emissions, with zero-

Downloaded 30 Jan 2007 to 192.84.145.254. Redistribution subject to AIP license or copyright, see http://jap.aip.org/jap/copyright.jsp

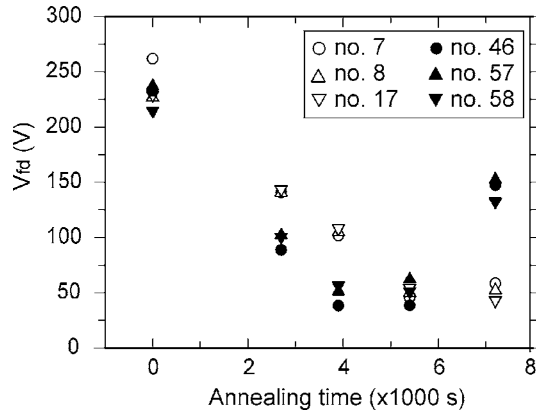

FIG. 5. Full depletion voltage V_{fd} plotted as a function of the annealing time for all the samples studied in this work.

field activation energies of 0.07 eV ($TD^{0/+}$) and 0.15 eV ($TD^{+/++}$), have been detected by DLTS in Czochralski silicon.[28–30] These lines represent the total response of the whole distribution of cluster sizes. The identification of these defects can in principle also be performed through different spectroscopic techniques, such as TSC. As a matter of fact, the feasibility of the TSC technique to perform measurements at temperatures lower than 20 K has been recently demonstrated by the investigation of shallow levels in FZ high resistivity silicon.[31–33]

Note that at the very early stage of annealing studied in this work, the thermal double donor species TD0, TD1, and TD2, which are bistable, should be the dominant ones. They can exist in two configurations: one (A) is associated with the double donor discussed above, while the other (B) is neutral. In configuration (B) the electrons are strongly bound to the center and the ionization energy exceeds the energy gap.[34–37] Only configuration (A) can be observed by DLTS, and the fraction of TDs frozen in this configuration depends on the Fermi level position during the cooling procedure.[38] Configuration (B) becomes stable only in *n*-type silicon if $E_F > E^{0/++}$ ($E_c - E^{0/++}$=0.45, 0.32, and 0.22 eV in the case of TD0, TD1, TD2 respectively). In this work we deal only with high resistivity samples whose starting material is *p* type and whose effective doping never exceeds $N_{eff} \sim 5 \times 10^{12}$ cm^{-3}, even after type inversion. Moreover cooling procedures are always carried out with an applied reverse bias, thus depleting the junction from free carriers. As a result we can expect almost all the TDs to emit from configuration (A) during TSC and *I*-DLTS measurements.

The TSC spectra of a diode (No.57) before any annealing and after 120 min heating at 430 °C are shown in Fig. 6. After the annealing treatment two intense peaks are observed at 25 K and 55 K, corresponding to emissions $TD^{0/+}$ and $TD^{+/++}$, respectively. On the contrary, before the thermal treatment, the same peaks are visible but with very weak amplitudes.

Various TSC spectra measured with different reverse biases are shown in Fig. 7. It is evident that the peaks shift at lower temperatures when the V_{rev} is increased, according to the Poole-Frenkel (PF) barrier lowering. Corresponding to each peak we can calculate the activation energy E by a best

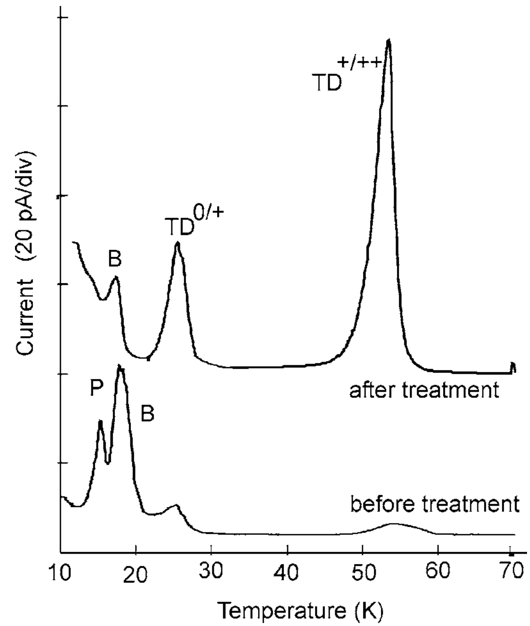

FIG. 6. Six TSC spectra of a MCz Si diode prior to any annealing and after the last thermal treatment (120 min at 430 °C). Reverse bias is V_{rev}=10 V, and heating rate is β=0.1 K/s.

fit procedure, thus obtaining the energy shifts $\Delta E = E_0 - E$, E_0 being the extrapolated zero-field activation energy. An example of peak fitting is shown in Fig. 8. As a first approximation, the energy shifts ΔE are related to the electric field F at the donor site by the following relation:[39,40]

$$\Delta E(F) = \left(\frac{Zq^3 F}{\pi \varepsilon \varepsilon_0} \right)^{1/2} = \alpha F^{1/2}. \qquad (1)$$

Here Z is the charge state of the emitting center: Z=1 for $TD^{0/+}$ transition and Z=2 for $TD^{+/++}$. According to this equation, $\alpha \cong 0.22$ meV(cm/V)$^{1/2}$ if Z=1, and $\alpha \cong 0.31$ meV(cm/V)$^{1/2}$ if Z=2. This simple formula accounts for one dimensional enhanced emission, which somewhat overestimates the barrier lowering of a three dimensional Coulombic well. According to this model, the plot of ΔE vs $F^{1/2}$ should give a straight line with slope α. In our analysis, the average value of electric field in the depleted region has been obtained as $F \cong V_{rev}/x_d$, where x_d is the depletion depth. The resulting TDs signatures and α values are in good agreement with the existing literature.[28–30] For $TD^{0/+}$ we found E_0=75±5 meV, $\sigma = 4 \times 10^{-14}$ cm^2, and α =0.3 meV(cm/V)$^{0.5}$. For $TD^{+/++}$ we found E_0=170±5 meV, $\sigma = 2 \times 10^{-12}$ cm^2, and α=0.2 meV(cm/V)$^{0.5}$.

Figure 9 shows the *I*-DLTS measurements carried out on the same diodes of Fig. 6, before and after 120 min of annealing. Before annealing the only visible spectral component is the one related to boron. After the thermal treatment the two TDs peaks are clearly observed. TD signatures obtained by TSC analysis are consistent with these measurements too.

Evidence of space charge sign inversion due to overcompensation of boron with TDs can be obtained by measuring the current transients at different temperatures. Nonmonotonic current transients are in fact produced by type inversion of the space charge,[26] which can take place during the emis-

Downloaded 30 Jan 2007 to 192.84.145.254. Redistribution subject to AIP license or copyright, see http://jap.aip.org/jap/copyright.jsp

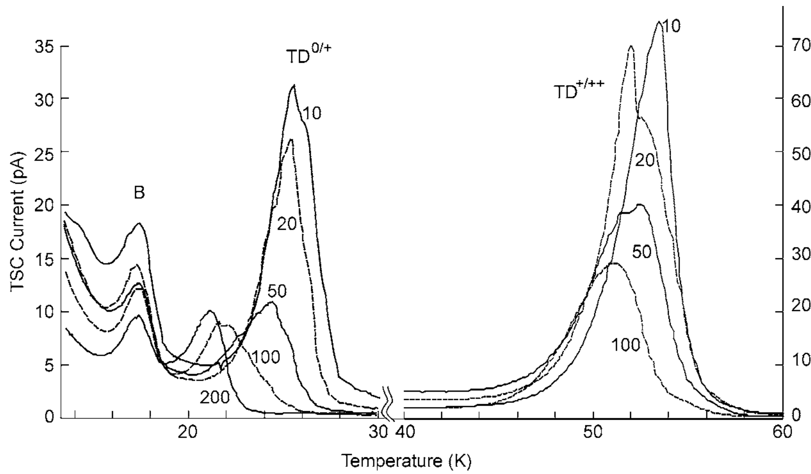

FIG. 7. TSC spectra measured with different reverse biases, showing peaks related to TDs emissions. The two temperature ranges corresponding to the TDs peaks are shown.

sion from an energy level such as those related to TDs. When this happens, if $V_{rev} < V_{fd}$, the active volume increases during the transient, reaches the total volume, and then decreases, producing a nonmonotonic current pulse shape. By measuring the temperature range in which the current transient shape is nonmonotonic, it is possible to infer quite precisely which energy level is responsible for type inversion. We have investigated our diodes with this technique in the temperature range close to the two TD peaks. Before thermal treatments, current transients are monotonic in the entire temperature range investigated by us. This means that the space charge, which is initially negative, as it is settled by boron, does not change sign during electron emissions $TD^{0/+}$ and $TD^{+/++}$. After the last thermal treatment, the current transient exhibits a nonmonotonic shape if the temperature is close to the value $T=65$ K, in proximity of the emission $TD^{+/++}$. Results are shown in Fig. 10, and can be explained as follows: when the temperature is close to 65–70 K, immediately after the filling pulse, TD levels are filled with electrons, and ρ is negative, due to boron doping. Subsequently, within few milliseconds, TDs become doubly ionized and produce a positive dominant contribution to the space charge, which determine the space charge sign inversion. This experimental evidence demonstrates that the second ionization $TD^{+/++}$ is responsible of the change of ρ sign observed by TCT. This also implies that the thermal donor's concentration n_{TD} is still smaller than the boron concentration $[B]=2 \times 10^{12}$ cm^{-3} (otherwise sign inversion would take place during $TD^{0/+}$ emission), and that n_{TD} is larger than $[B]/2$ (otherwise sign inversion would never appear): $[B] > n_{TD} > [B]/2$.

In principle, information about the concentration of emitting levels can be obtained from the amplitude of TSC or *I*-DLTS spectra. This can be easily accomplished if the active volume is constant during the emission. This is not our case, because carrier emission from TD levels causes a huge modification of N_{eff}, resulting in a change of depletion depth and active volume. In addition, the occurring of field enhanced emission introduces additional uncertainty on the relationship between peak amplitude and center's population. Nevertheless, it is possible to explain qualitatively the amplitude

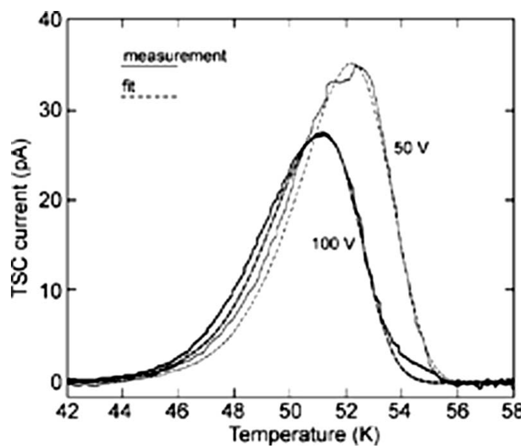

FIG. 8. TSC spectra showing Poole-Frenkel effect and $TD^{+/++}$ peak fitting. The measurements are denoted by solid lines, and fits by dashed lines. Thick lines refer to $V_{rev}=100$ V and thin lines to $V_{rev}=50$ V. Fits have been calculated according to standard TSC analysis, and the discrepancy with respect to the measured spectra is due to the space charge modulation occurring during carrier emission.

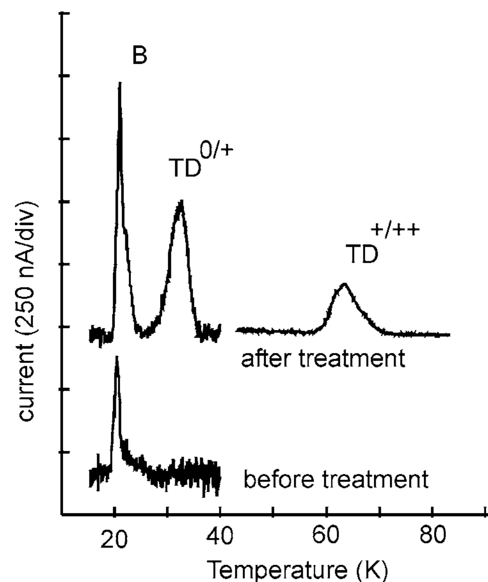

FIG. 9. I-DLTS spectra measured before (lower plot) and after a 120 min thermal treatment (upper plot). Sampling times are $t_1=20$ ms and $t_2=90$ ms, the reverse bias is $V_{rev}=10$ V, and the deep level excitation is obtained by a forward pulse of $t_{fill}=10$ ms duration.

Downloaded 30 Jan 2007 to 192.84.145.254. Redistribution subject to AIP license or copyright, see http://jap.aip.org/jap/copyright.jsp

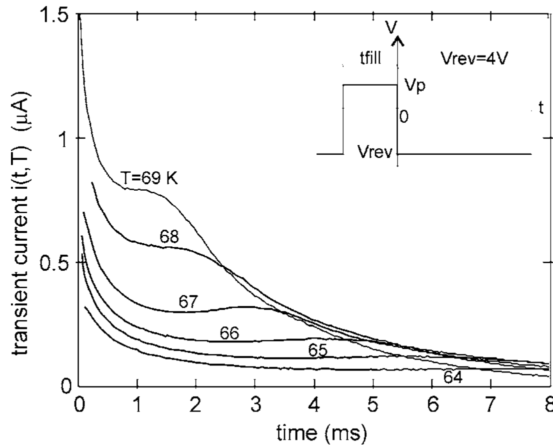

FIG. 10. Current transients measured, after 120 min at 430 °C, close to the temperature of $TD^{+/++}$ I-DLTS peak. The energy level excitation is obtained by a forward pulse of $t_{fill}=10$ ms duration. $V_{rev}=4$ V. The carrier injection procedure is explained in detail in the insert.

of the low-field TSC peaks related to TDs. The amplitude of the $TD^{0/+}$ and $TD^{+/++}$ peaks is proportional to the concentration of those donors populated by low temperature injection (which is the same for the two peaks) and to the volume of the depleted region. The amplitude of the $TD^{+/++}$ peak at 55 K is higher than the amplitude of the $TD^{0/+}$ one because N_{eff} diminishes after the $TD^{0/+}$ emission at 25 K, thus determining an increase of the active volume. Such an explanation does not hold for *I*-DLTS peaks because the current transient due to $TD^{+/++}$ emission is nonmonotonic. As discussed in detail in Ref. 26 this effect produces a strong distortion of the $TD^{+/++}$ peak which makes any comparison meaningless with the amplitude of the $TD^{0/+}$ one.

C. Thermal donor's formation rate

Our results give a direct proof of the TD's activation via isothermal annealing in MCz Si. In this paragraph, we wish to discuss TD's formation rate as a function of annealing time and initial oxygen concentration by comparing earlier works on low resistivity silicon with our results. According to these studies,[41,42] the initial rate of donor formation (dn_{TD}/dt) at 450 °C is almost linear with annealing time and proportional to the fourth power of the grown-in interstitial oxygen concentration $[O_i]$. Using simple kinetic arguments, this result was considered to provide evidence that the core of TD defects contains four oxygen atoms. In Ref. 11 a simplified aggregation model of oxygen thermal donors is described, based upon existing experimental data. The concentration of thermal donors is given by the law:

$$n_{TD}(t) = k_t\left\{[O_i]\left[1+\frac{2}{3}D_i t[O_i]^{2/3}\right]^{-2/3}\right\}^x t^{1.02}, \quad (2)$$

with D_i diffusivity of interstitial oxygen, t annealing time, and $k=4.61\times10^{-52}$. The proportionality of n_{TD} with $t^{1.02}$ is discussed in detail in Ref. 43, where this model has been tested with low resistivity Cz Si ($[O_i]\cong 7\times10^{17}$ cm^{-3}), doped with $2-8\times10^{14}$ cm^{-3} P or B and annealed at 450–470 °C. For annealing times up to 6×10^5 s, the TD concentration was found to increase almost linearly with increasing annealing time. In more recent works, these measurements have been extended to a wider range of temperatures (350 °C $<T<$ 500 °C) and modeling have been further improved.[12] These latter results showed that in the range of 350–400 °C a second-power dependence ($x=2$) is more appropriate, suggesting that the dominant mechanism controlling the formation of TDs is presumably limited by the rate of oxygen dimer's (O_{2i}) formation. At higher temperatures, oxygen agglomerates would tend to dissociate on a time scale close to that required to cause a measurable increase of n_{TD} and this would bring a superlinear increase of the power exponent x. The values $x=3.5$ and 9 were estimated, respectively, at 450 and 500 °C.

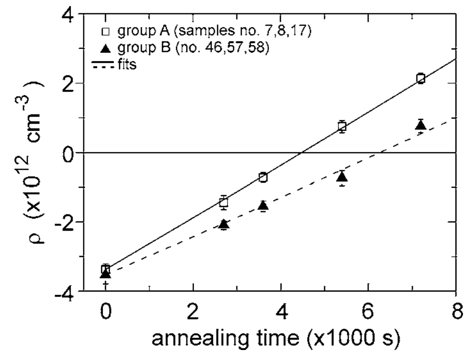

FIG. 11. Space charge density ρ vs annealing time. Trends of sets A and B have been simulated using Eq. (2) considering a fixed annealing temperature close to 430 °C and an initial interstitial oxygen concentration $[O_i]$ which can vary along the wafer.

Our measurements of TCT, coupled with TSC and DLTS analyses, show that a space charge sign inversion occurs in the initially *p*-type Si material due to the formation of TD aggregates. The initial decrease of V_{fd} with time shown in Fig. 5 is actually due to the compensation of boron with an increasing concentration of the TDs. This decreasing trend is followed by a V_{fd} increase when the TDs start to overcompensate the B doping and the inversion of the space charge sign occurs. We note that samples, cut from the same wafer regions, show a similar trend of V_{fd}. To evidence this effect N_{eff} has been evaluated from the mean value of full depletion voltage $\langle V_{fd}\rangle$, measured for samples of the same group, as $N_{eff}=2\varepsilon\langle V_{fd}\rangle/(qW^2)$. In this formula ε indicates the absolute dielectric constant, and W is the thickness of the sample. The plot of $\rho=N_{eff}\eta$ as a function of the annealing time is shown in Fig. 11. The linear increase of ρ from negative to positive values can be explained considering that, in agreement with Ref. 43, the concentration of TDs is increasing almost linearly with annealing time, up to the overcompensation of the B dopants.

The two sets A and B are characterized by different activation rates: samples from the central part of the wafer have a slope value 30% higher than those cut closer to the wafer periphery. To discuss this effect we simulated the $\rho(t)$ curves by means of Eq. (2). The effective density in the space charge has been calculated as

$$\rho = \eta N_{eff}(t) = 2n_{TD}(t) - N_B. \quad (3)$$

The interstitial oxygen diffusivity D_i, which appears in Eq. (2), has been calculated as $D_i=D_\infty e^{-E_a/kT}$, with D_∞

Downloaded 30 Jan 2007 to 192.84.145.254. Redistribution subject to AIP license or copyright, see http://jap.aip.org/jap/copyright.jsp

$=0.13$ cm^2/s and $E_a=2.53$ eV, in agreement with Ref. 11. The interstitial oxygen concentration $[O_i]$ is used as the free parameter. The possibility of small temperature variations (±0.5 °C) around the nominal value of 430 °C has been taken into account, and the value of the exponential factor x has been varied with temperature according to Ref. 12. The two best fits of the curves shown in Fig. 11 have been obtained with same annealing temperature (429.5 °C), slightly lower than the nominal one, using $[O_i]=4.4\times10^{17}$ cm^{-3} (for samples coming from set A) and $[O_i]=4.8\times10^{17}$ cm^{-3} (for samples coming from set B). Thus, at this temperature, the different trends of samples from sets A and B can be well accounted for by the $\pm0.2\times10^{17}$ cm^{-3} uncertainty in the initial oxygen concentration measured by SIMS analysis.[24] Note that, according to Eq. (3), the N_{eff} value determined from TCT measurements gives a TD concentration ranging from $n_{\mathrm{TD}}=2.3\times10^{12}$ cm^{-3} in the peripheral region to $n_{\mathrm{TD}}=2.8\times10^{12}$ cm^{-3} in the central region. These values fit well to those found with TSC and DLTS measurements, which gave $n_{\mathrm{TD}}=2-4\times10^{12}$ cm^{-3}.

By concluding this section we wish to note that, as the formation of TD is very sensitive to the precise value of the exponential factor x, which in turn depends critically on the annealing temperature T, even small variations of the annealing temperature might influence dramatically the rate of TD formation. This phenomenon deserves further investigations in order to assess the procedure of TD activation outlined in this work.

IV. CONCLUSIONS

This work presents a thorough study of thermal donor activation via isothermal annealing at 430 °C, up to 120 min, on high resistivity magnetic Czochralski silicon. The study has been carried out on diodes made from initially p-type material. Transient current technique (TCT) has been used to measure the full depletion voltage, effective doping concentration, and sign of the space charge after process and at each annealing step. Thermal donors have been directly observed by means of current deep level transient spectroscopy (I-DLTS) and by thermally stimulated currents (TSCs). Activation energies and effective cross sections have been evaluated for single and double emissions: $TD^{0/+}$ ($E=75\pm5$ meV, $\sigma=4\times10^{-14}$ cm^2) and $TD^{+/++}$ ($E=170\pm5$ meV, $\sigma=2\times10^{-12}$ cm^2). Our results evidence that the activation of TDs is responsible for the progressive compensation of the boron doping during annealing. After the longest thermal treatment, overcompensation occurred and a change of the space charge sign was observed. At the longest annealing time, thermal donor concentrations estimated by us are $n_{\mathrm{TD}}\cong2.3-2.8\times10^{12}$ cm^{-3}. Consistently, current transient measurements revealed that the second ionization of thermal donors $TD^{+/++}$ is indeed responsible for the inversion of space charge sign.

We used our experimental data to validate a model of thermal donor formation rate proposed in earlier works for low resistivity (1–100 Ω cm) Cz silicon.[11,12] Our results confirm this model, showing that it can be extended to the 1–100 kΩ cm resistivity range. Our work also demonstrate that the annealing procedure is a simple and effective way to obtain very high resistivity MCz Si both of n and p types from the same starting low resistivity material. Nonetheless, we showed that a strict control of the annealing parameters and of the initial interstitial oxygen concentration is necessary to obtain reproducible results. In fact, small fluctuations in the initial interstitial oxygen concentration along the wafer size, or slight changes in the annealing temperature, can introduce significant uncertainties in the rate of thermal donor formation.

ACKNOWLEDGMENTS

This work has been performed in the framework of the CERN RD50 Collaboration, it has been supported in part by the Academy of Finland, and, in Italy, by the SMART project of INFN, 5th Commission. The authors wish to thank Andrea Baldi and Dr. Antonio de Sio from University of Florence for helpful technical support.

[1] G. Batignani *et al.*, Nucl. Instrum. Methods Phys. Res. A **518**, 569 (2004).
[2] P. P. Allport *et al.*, IEEE Trans. Nucl. Sci. **48**, 1007 (2001).
[3] C. M. Sun, D. J. Han, L. Y. Sheng, X. R. Zhang, H. J. Zhang, R. Yang, L. Zhang, and B. J. Ning, Nucl. Instrum. Methods Phys. Res. A **547**, 437 (2005).
[4] T. Abe and W. Qu, Proc.-Electrochem. Soc. **2000–17**, 491 (2000).
[5] T. Sinno, E. Dornberger, W. von Ammon, R. A. Brown, and F. Dupret, Mater. Sci. Eng., R. **28**, 149 (2000).
[6] J. Härkönen *et al.*, Nucl. Instrum. Methods Phys. Res. A **514**, 173 (2003).
[7] V. Savolainen *et al.*, J. Cryst. Growth **243**, 243 (2002).
[8] B. A. Andreev, V. V. Emtsev, D. I. Kryzhkov, D. I. Kuritsyn, and V. B. Shmagin, Phys. Status Solidi B **235**, 79 (2003).
[9] M. Pesola, J. L. Young, J. von Boehm, M. Kaukonen, and R. M. Nieminen, Phys. Rev. Lett. **84**, 5343 (2000).
[10] R. Jones, J. Coutinho, S. Oberg, and P. R. Briddon, Physica B **308–310**, 8 (2001).
[11] W. Wijaranakula, Appl. Phys. Lett. **59**, 1608 (1991).
[12] C. A. Londos, M. J. Binns, A. R. Brown, S. A. McQuaid, and R. C. Newman, Appl. Phys. Lett. **62**, 1525 (1993).
[13] R. C. Newman, J. Phys.: Condens. Matter **12**, R335 (2000).
[14] R. C. Newman, J. H. Tucker, N. G. Semaltianos, E. C. Lightowlers, T. Gregorkiewicz, I. S. Zevenbergen, and C. A. J. Ammerlaan, Phys. Rev. B **54**, R6803 (1996).
[15] J. Härkönen *et al.*, Nucl. Instrum. Methods Phys. Res. A **541**, 202 (2005).
[16] V. Eremin, N. Strokan, E. Verbitskaya, and Z. Li, Nucl. Instrum. Methods Phys. Res. A **372**, 388 (1996).
[17] D. V. Lang, J. Appl. Phys. **45**, 3023 (1974).
[18] B. W. Wessels, J. Appl. Phys. **47**, 1131 (1976).
[19] C. H. Hurtes, M. Boulou, A. Mitonneau, and D. Bois, Appl. Phys. Lett. **32**, 821 (1978).
[20] M. G. Buehler, Solid-State Electron. **15**, 69 (1972).
[21] P. Blood and J. W Orton, *The Electrical Characterization of Semiconductors: Majority Carriers and Electron States* (Academic, London, 1992).
[22] J. Frenkel, Phys. Rev. **54**, 647 (1938).
[23] S. D. Ganichev *et al.*, Phys. Rev. B **61**, 10361 (2000).
[24] G. Pellegrini, J. M. Rafı, M. Ullán, M. Lozano, C. Fleta, and F. Campabadal, Nucl. Instrum. Methods Phys. Res. A **548**, 355 (2005).
[25] Z. Li, V. Eremin, N. Strokan, and E. Verbitskaya, IEEE Trans. Nucl. Sci. **40**, 367, (1993).
[26] D. Menichelli, M. Scaringella, M. Bruzzi, I. Pintilie, and E. Fretwurst, Phys. Rev. B **70**, 195209 (2004).
[27] W. Gotz, G. Pensl, and W. Zulehner, Phys. Rev. B **46**, 4312 (1992).
[28] L. C. Kimerling and J. L. Benton, Appl. Phys. Lett. **39**, 410 (1981).
[29] W. Keller and K. Wunstel, Appl. Phys. A **31**, 9 (1983).
[30] K. Wada and N. Inoue, J. Appl. Phys. **57**, 5145 (1985).
[31] E. Borchi, M. Bruzzi, S. Pirollo, and S. Sciortino, J. Phys. D **31**, L93 (1998).
[32] E. Borchi, M. Bruzzi, Z. Li, and S. Pirollo, IEEE Trans. Nucl. Sci. **47**, 1474 (2000).

Downloaded 30 Jan 2007 to 192.84.145.254. Redistribution subject to AIP license or copyright, see http://jap.aip.org/jap/copyright.jsp

[33] E. Borchi, M. Bruzzi, Z. Li, and S. Pirollo, J. Phys. D **33**, 299 (2000).
[34] Y. A. I. Latushko, L. F. Makarenko, V. P. Markevich, and L. I. Murin, Phys. Status Solidi A **93**, K181 (1986).
[35] V. P. Markevich, L. F. Makarenko, and L. I. Murin, Phys. Status Solidi A **97**, K173 (1986).
[36] A. Chantre, Appl. Phys. A **48**, 3 (1989).
[37] L. I. Murin, V. P. Markevich, J. L. Lindstroem, and M. Kleverman, Physica B **340–342**, 1046 (2003).
[38] A. Chantre, Appl. Phys. Lett. **50**, 1500 (1987).
[39] J. L. Hartke, J. Appl. Phys. **39**, 4871 (1968).
[40] P. A. Martin, B. G. Streetman, and K. Hess, J. Appl. Phys. **52**, 7409 (1981).
[41] W. Kaiser, Phys. Rev. **105**, 1751 (1957).
[42] W. Kaiser, H. L. Frisch, and H. Reiss, Phys. Rev. **112**, 1546 (1958).
[43] W. Wijaranakula and J. H. Matlock, J. Electrochem. Soc. **137**, 1964 (1990).

Downloaded 30 Jan 2007 to 192.84.145.254. Redistribution subject to AIP license or copyright, see http://jap.aip.org/jap/copyright.jsp